Quantum disordering versus melting in Lennard-Jones clusters

Jason Deckman and Vladimir A. Mandelshtam

Department of Chemistry, University of California at Irvine, Irvine, California 92697, USA

(Received 7 December 2008; published 25 February 2009)

The ground states of Lennard-Jones clusters for sizes up to $n=147$ are estimated as a function of the de Boer quantum delocalization length Λ, and the $n-\Lambda$ "phase diagram" is constructed. The increase in Λ favors more disordered and diffuse structures over more symmetric and compact ones, eventually making the liquidlike motif most energetically favorable. The analogy between the quantum- and thermally-induced structural transitions is explored.

The Lennard-Jones (LJ) clusters exhibit rich thermodynamic properties and display complex behavior that is sensitive to their size and temperature (see Refs. [1–6] for examples). Both classical and quantum LJ clusters have been studied very extensively in the last several decades. Even without taking into account the quantum effects these systems have always made accurate simulations challenging due to the high complexity of their potential energy landscapes. Consequently, these studies have stimulated the development of various numerical techniques, such as Monte Carlo or molecular dynamics, or various algorithms of global optimization, etc.

With some notable exceptions, for sizes $n \lesssim 1000$ the global minima structures of LJ_n clusters are dominated by the icosahedral motif [7,8], while the closed-packed structures start to be favorable only around $n \sim 10^5$ [9]. An icosahedral structure may be characterized by the existence of a complete icosahedral core ($n=13,55,147,\ldots$) surrounded by an incomplete overlayer, which can adopt two different packings: the anti-Mackay ($n=14-30,56-81,85,\ldots$) or Mackay ($n=31-55,82-147,\ldots$). There are several exceptions of clusters ($n=74-76,98,102-104,\ldots$) that adopt nonicosahedral structures as their global minimum configuration.

At finite temperatures local energy minima start to contribute to the equilibrium properties of the cluster. The presence of different structural motifs that may be favorable for certain ranges of the parameters (n or T) gives rise to size- or temperature-induced structural transitions, resulting from competition between the energy and entropy. Even for relatively small sizes ($n \sim 20$) the number of the thermodynamically relevant minima for a LJ_n cluster is already very large and keeps increasing exponentially with size. Moreover, these minima are often separated by large barriers leading to severe sampling problems. The replica-exchange Monte Carlo method [10] is commonly employed to deal with such problems. The first successful application of the latter to a LJ cluster ($n=38$) had been reported relatively recently [2]. Despite an apparent superiority of the methodology, at the time this calculation seemed to be heroic. More recently a series of replica-exchange calculations covering a wide range of sizes was carried out [3–6].

Notwithstanding the difficulties of a classical simulation of LJ clusters, accurately modeling the quantum effects is further challenging. Calculations using path integral Monte Carlo (PIMC) methods, when converged, provide essentially exact results. However, when trying to accurately describe structural transformations using PIMC, the computation times can be excessively long and increase dramatically with decreasing temperature. Because in the case of a structural transition at least two basins of attraction, usually separated by a large energy barrier, must be sampled, regardless of whether the quantum effects are included in the simulation or not, the sampling problem already exists. In the PIMC framework this problem is alleviated by the presence of an additional (short) time scale associated with the path variables describing the shape of the path. Strong quantum effects (such as quantum delocalization and/or tunneling), as, e.g., in the helium systems, may effectively remove the ergodicity problem. However, it is the intermediate quantum regime, which is most challenging for accurate quantum simulations, especially for systems that undergo structural transformations at low temperatures. Examples of such systems include neon clusters, and, very likely, hydrogen clusters. Perhaps not surprisingly, the Ne_{13} cluster is the largest neon system undergoing a low-temperature ($T \sim 10$ K) structural change, for which a converged heat capacity curve computed by the PIMC was reported [11]. Larger neon clusters, e.g., Ne_{39}, which undergo low-temperature structural changes [12], seem at the moment too difficult to be treated accurately by PIMC [13]. As yet another example, we believe that the recent attempt [14] to compute the ground states of $(H_2)_n$ and $(D_2)_n$ clusters using a variant of the PIMC methodology seem to fail to accurately characterize the size-induced structural changes in these systems. In another paper [15] the diffusion Monte Carlo methodology was used to also compute the ground states of $(H_2)_n$ clusters, but the results are in disagreement with Ref. [14] and are possibly nonconverged as well.

A rare gas atomic system or a molecular system (e.g., a hydrogen cluster) interacting through van der Waals forces can be mapped to a model LJ_n system with a particular value of the de Boer quantum delocalization length $\Lambda = (\hbar/\sqrt{m\epsilon})/\sigma$, where m is the particle mass, and ϵ and σ are the parameters of the LJ pair potential,

$$U(r) = 4\epsilon[(\sigma/r)^{12} - (\sigma/r)^6].$$

Λ is an effective measure of delocalization of the ground-state wave function relative to the interatomic distance. Although only particular discrete Λ values can be realized in nature, by looking at the properties of LJ_n cluster as a func-

tion of continuously varying Λ one can gain insights, which are not available otherwise.

Faced with the above difficulties, for weakly quantum systems, it seems to be practical to use approximate methods that have better sampling properties, but may still account for the quantum effects adequately. One such method is the harmonic approximation (HA), which can be used for estimation of the ground-state energies and wave functions for the entire range of Λ. As an example, Ref. [9] presents a HA analysis of the ground-state structures of LJ clusters corresponding to different rare gas atomic clusters. While the HA is straightforward to implement and it may be adequate for nearly classical cases, as e.g., xenon ($\Lambda \sim 0.01$), krypton ($\Lambda \sim 0.016$) or argon ($\Lambda \sim 0.03$), in a more quantum regime, e.g., corresponding to neon ($\Lambda = 0.095$), the HA predictions can be very crude [16,17].

Our method of choice is the variational Gaussian wave packet (VGW) method [12,16,17]. The VGW is exact for a harmonic potential, while it is manifestly approximate for a general anharmonic potential, yet this method demonstrated its practicality, specifically, for the case of Ne_{38} [16], for which the VGW energies agreed very well with those computed by the PIMC method. In our previous work [17] the VGW method was applied to investigate the LJ_{31-45} clusters, which, with the exception of LJ_{38}, possess Mackay global energy minima. It was shown that the quantum delocalization always induces the Mackay$\rightarrow$anti-Mackay (M$\rightarrow$aM) transition. Consequently, a "phase diagram" showing the stability ranges of the two structural motifs was constructed.

The present Brief Report extends the ground-state calculations of LJ_n clusters up to $n=147$, the largest size of a three-layer cluster with icosahedral symmetry. As n increases the VGW calculations become increasingly more time-consuming. In order to reduce the computational burden only the following sizes were included: $n=31-55,60,65,70,$ $75-77,80,82-90,95,98,100,102-104,105,110,115,120,$ $125,130,135,140,145,147$. LJ_{82} is the smallest cluster with Mackay global energy minimum and 55-atom core. The sizes, $n=38,75-77,98,102-104$, include all the cases of nonicosahedral global energy minima, namely, truncated octahedron (O_h) for $n=38$, Marks decahedra (D_h) for $n=75-77,102-104$, and tetrahedron (T_h) for $n=98$.

The VGW method for estimating the cluster ground-state energy and structure is based on minimization of the energy functional,

$$E = \langle \Psi | \hat{H} | \Psi \rangle \langle \Psi | \Psi \rangle^{-1}, \tag{1}$$

with the trial wave function (or VGW) chosen in the form

$$\Psi(\mathbf{q}, \mathbf{G}, \gamma) = \exp\left[-\frac{1}{2}(\mathbf{r} - \mathbf{q})^{\mathrm{T}} \mathbf{G}^{-1}(\mathbf{r} - \mathbf{q}) + \gamma \right], \tag{2}$$

where the variational parameters are: the $3n \times 3n$ real symmetric matrix $\mathbf{G}$, real $3n$-vector $\mathbf{q}$, and factor γ.

For each cluster size the replica-exchange method [10] (using the system potential energy) is utilized to sample the configuration space. Every once in many Monte Carlo steps a configuration is selected from one of the random walks for (quantum) quenching to yield a stationary VGW that mini-
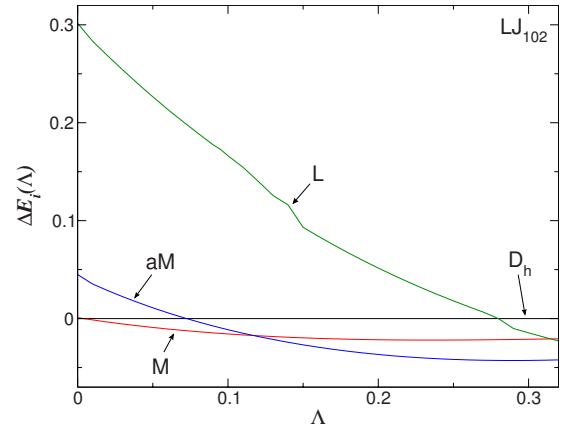

FIG. 1. (Color online) Correlation diagram for LJ_{102} showing the relative energies, $\Delta E_i(\Lambda) := [E_i(\Lambda) - E_o(\Lambda)]/n$, as a function of Λ for four quantum states, each being the lowest-energy state for one of the four different structural motifs. $i=0$ corresponds to the global classical energy minimum. The structural transitions occur where the curves intersect each other.

mizes the energy functional (1), given the Gaussian constraints (2). Typically the quenched configuration is found in the vicinity of the initial configuration. The energy of the particular stationary solution is then compared to the energies of the solutions found previously. Configurations of sufficiently low energy are retained to be used later to produce energy correlation diagrams. The latter consist of the energy curves $E_i(\Lambda)$ generated for a range of Λ using all the retained configurations. Given a value of Λ, the lowest energy configuration is then assumed to represent the cluster ground state. More details of the method can be found in Ref. [17] and in a forthcoming paper.

The analysis of all the correlation diagrams revealed several distinct structural motifs that turned out to be stable within certain ranges of Λ. Those include the Mackay (M), anti-Mackay (aM), and liquidlike (L) structures, which are generic for all clusters considered. In addition, for clusters with nonicosahedral global energy minima, the corresponding structural motifs remain stable within certain (sometimes very small) ranges of Λ values. One such example is the LJ_{102} cluster, which in addition to the two generic transitions (M$\rightarrow$aM and aM$\rightarrow$L) undergoes a $\mathrm{D}_h \rightarrow$M transition at $\Lambda \approx 4.1 \times 10^{-3}$. The corresponding correlation diagram, which only shows one energy curve per structural motif, is given in Fig. 1. The four ground-state structures involved in this figure are shown in Fig. 2. (We use reduced variables for energy and temperature, i.e., the energy is measured in units of $[\epsilon]$ and temperature, in units of $[\epsilon/k_B]$.)

All the identified Λ values corresponding to the structural transformations in LJ_n clusters were used to produce the $n - \Lambda$ "phase diagram" (see Fig. 3), which shows the stability regions for different structural motifs as a function of n and Λ. The size-temperature ($n-T$) phase diagram of the classical ($\Lambda=0$)LJ_n clusters is also shown for comparison. The latter diagram was constructed based on the data from Refs. [4,6]. There is a striking resemblance between the two diagrams, in which one can find the same structural motifs stable over certain ranges of parameters. Structurally, motifs
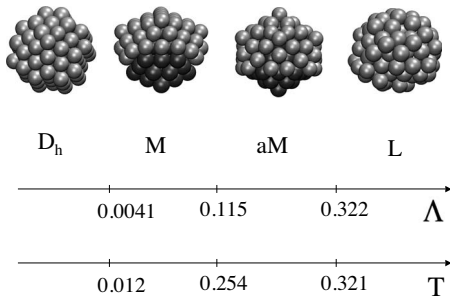
FIG. 2. The four configurations of LJ_{102} cluster involved in Fig. 1. The darker color is used to identify the core atoms in the Mackay and anti-Mackay structures. The Λ and T axes identify the values of the corresponding structural transitions for, respectively, quantum ($T=0$) and classical ($\Lambda=0$) cases.

denoted by the same symbol are indistinguishable. Note though that unlike the high-temperature liquid configurations in the classical diagram, the quantum "liquidlike" structures, although being disordered, are completely frozen. The quantum-induced aM→L ("order-disorder") transition in the present case has nothing to do with quantum tunneling, nor does it involve any superfluidity as the exchange symmetries are not taken into account within the VGW approximation.

Quantum delocalization (as well as the temperature increase) always stabilizes the anti-Mackay relative to the Mackay motif. Further increase in Λ (or T) eventually destabilizes the anti-Mackay structure resulting in the least-ordered liquidlike structure. However, for small, two-layer clusters, we were not able to clearly distinguish between liquidlike and anti-Mackay structures. The probable reason is that the 13-atom icosahedral "core" is typically not unique for an anti-Mackay structure (i.e., there may be several 13-atom subclusters having the same arrangement of the complete icosahedron), while the 12-atom coordination is also characteristic of liquidlike structures. (This problem may be resolved in the future if an appropriate order parameter is found.) A similar difficulty was encountered when analyzing the temperature-induced structural changes in classical LJ_n clusters [4], for which the liquid and anti-Mackay structural motifs could clearly be distinguished only for three-layer clusters ($55 < n \leq 147$), the existence of the well-ordered complete-icosahedral 55-atom core being a unique property of the icosahedral motif. For the latter clusters the heat capacity curve displays a sharp peak at the temperature of the aM→L transition (also identified as the "core melting transition"). For the classical two-layer LJ clusters only the M→aM transition can be identified unambiguously and is always accompanied by a sharp heat capacity peak. Furthermore, this peak changes gradually as a function of cluster size and continues into the size region ($n>45$), where the two-layer anti-Mackay structures do not exist. That is, if one follows the M→aM transition as a function of cluster size, starting with small sizes ($n\geq 31$), it gradually changes in character, so that for larger clusters it is perhaps more representative of just "cluster melting." Figure 4 shows two examples of anti-Mackay ground-state structures for $n=115$ (the stability range is $\Lambda \in [0.1116, 0.3540]$) and $n=147$ ($\Lambda \in [0.3102, 0.4121]$). Although the largest structure with a
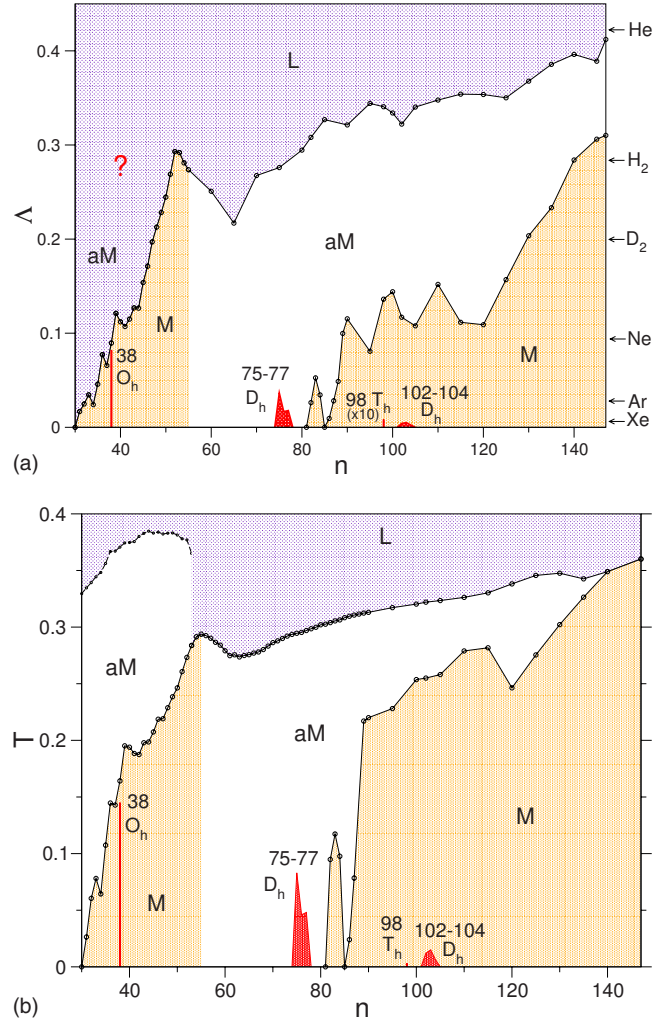

FIG. 3. (Color online) The $n-\Lambda$ phase diagram (top) showing the stability ranges for the ground-state structures of quantum LJ_n clusters ($n=30-147$). The points are connected for better visualization. The bar for $n=98$ is scaled by a factor of 10, also for better visualization. The question mark indicates the difficulty in distinguishing between anti-Mackay and liquidlike structures for two-layer clusters. Bottom: the corresponding $n-T$ phase diagram, which bears similarity to the top figure. The latter diagram was constructed using the data from Refs. [4,6].

single-anti-Mackay overlayer surrounding the 55-atom Mackay icosahedral core corresponds to LJ_{115} (having a perfect, nearly spherical shape), for $n>115$ structures with double-anti-Mackay overlayer can become energetically favorable and are easily identified, as in the case of LJ_{147}. Note also Ref. [5], where two temperature-induced structural transformations were observed for the classical LJ_{309} cluster, whose global minimum is a complete four-layer Mackay icosahedron. In the latter work the lower-temperature transition was interpreted as "surface roughening" of the overlayer surrounding the 147-atom Mackay icosahedral core.

For the lack of both a rigorous and simple method, one is often tempted to incorporate the quantum effects into the molecular dynamics simulations by using an "effective temperature." The comparison of the classical $n-T(\Lambda=0)$ and quantum $n-\Lambda(T=0)$ diagrams suggests that such a mapping
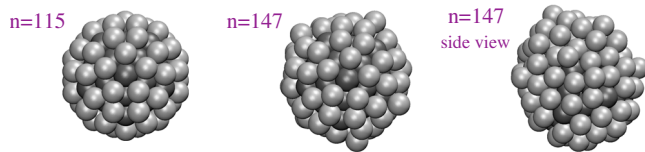
n=115   n=147   n=147
                  side view

FIG. 4. (Color online) Images of anti-Mackay structures of LJ$_{115}$ and LJ$_{147}$, each characterizing the ground state of the corresponding cluster stable over certain Λ range. $n=115$ is the largest size with 55-atom Mackay icosahedral core and anti-Mackay overlayer. For $n>115$ the extra atoms fill the fourth layer forming a double-anti-Mackay overlayer, which can be seen in the "side view."

exists on a certain qualitative level, although it is not universal. For example, in the $n-T(\Lambda=0)$ diagram the M$\rightarrow$L and M$\rightarrow$aM transition temperatures merge for $n\geq140$, while in the $n-\Lambda(T=0)$ diagram the M$\rightarrow$L and M$\rightarrow$aM transitions for the same size range occur at different values of Λ.

Another interesting parallel exists between the present $n-\Lambda$ diagram for the quantum LJ$_n$ clusters and $n-\rho$ diagram for the global minima structures of the classical Morse clusters [18,19], where the Morse pair potential is

$$U(r) = \epsilon \exp[\rho(1 - r\sigma)]\{\exp[\rho(1 - r/\sigma)] - 2\}$$

with ρ defining the range of the potential; the larger the ρ value the shorter the range. Increasing the range of the potential destabilizes the Mackay (relative to the anti-Mackay) structures. Further increase in the range eventually makes the liquid-like structures energetically most favorable. In view of this comparison we conclude that the quantum delocalization, besides making the effective pair interaction softer, also increases its range.

In conclusion, we believe that for the weakly quantum regime, which at least includes the neon clusters, our results are generally correct, but may only be qualitatively correct for the more quantum regime, perhaps starting with hydrogen clusters. When the quantum effects are sufficiently strong, the Gaussian approximation may fail to adequately describe the delocalized ground-state wave function. Moreover, it is believed that the particle exchange symmetry becomes important, at least for hydrogen clusters, and may even result in superfluidity [14], while this effect is completely ignored within the present approximation. At the same time, due to the sampling problems, the path-integral and related methods may be hard to apply in the weakly quantum regime, while they become much better suited for the strongly quantum regime.

[1] J. P. K. Doye, M. A. Miller, and D. J. Wales, J. Chem. Phys. **110**, 6896 (1999); **111**, 8417 (1999).

[2] J. P. Neirotti, F. Calvo, D. L. Freeman, and J. D. Doll, J. Chem. Phys. **112**, 10340 (2000); **112**, 10350 (2000).

[3] D. D. Frantz, J. Chem. Phys. **115**, 6136 (2001).

[4] V. A. Mandelshtam and P. Frantsuzov, J. Chem. Phys. **124**, 204511 (2006).

[5] E. G. Noya and J. P. K. Doye, J. Chem. Phys. **124**, 104503 (2006).

[6] V. A. Sharapov and V. A. Mandelshtam, J. Phys. Chem. A **111**, 10284 (2007).

[7] J. A. Northby, J. Chem. Phys. **87**, 6166 (1987).

[8] R. H. Leary, J. Glob. Optim. **11**, 35 (1997).

[9] J. P. K. Doye and F. Calvo, J. Chem. Phys. **116**, 8307 (2002).

[10] C. J. Geyer, in *Computing Science and Statistics*, Proceedings of the 23rd Symposium on the Interface, edited by E. M. Keramigas (Interface Foundation, Fairfax, 1991), pp. 156–163;

K. Hukushima and K. Nemoto, J. Phys. Soc. Jpn. **65**, 1604 (1996).

[11] C. Predescu, D. Sabo, J. D. Doll, and D. L. Freeman, J. Chem. Phys. **119**, 12119 (2003); **121**, 856 (2004).

[12] P. A. Frantsuzov, D. Meluzzi, and V. A. Mandelshtam, Phys. Rev. Lett. **96**, 113401 (2006).

[13] C. Predescu (private communication).

[14] J. E. Cuervo and P.-N. Roy, J. Chem. Phys. **128**, 224509 (2008).

[15] R. Guardiola and J. Navarro, Cent. Eur. J. Phys. **6**, 33 (2008).

[16] C. Predescu, P. A. Frantsuzov, and V. A. Mandelshtam, J. Chem. Phys. **122**, 154305 (2005).

[17] J. Deckman, P. A. Frantsuzov, and V. A. Mandelshtam, Phys. Rev. E **77**, 052102 (2008).

[18] J. P. K. Doye, D. J. Wales, and R. S. Berry, J. Chem. Phys. **103**, 4234 (1995).

[19] J. P. K. Doye and D. J. Wales, Science **271**, 484 (1996).